Appl Phys B
DOI 10.1007/s00340-008-3356-0

Applied Physics B
Lasers and Optics

Modulation enhancement of a laser diode in an external cavity

A. Waxman · M. Givon · G. Aviv · D. Groswasser · R. Folman

Received: 17 October 2008 / Revised version: 1 December 2008

Abstract We present experimental results demonstrating enhanced current modulation of an antireflection-coated edge-emitting laser diode placed in an external cavity. By eliminating the internal cavity of the laser diode and matching the external cavity free spectral range to the modulation frequency we have increased the modulation response up to nearly complete carrier suppression. We demonstrate the tunability of this enhanced modulation over a range of more than 3 GHz. The power of the modulated beam has been measured to be 10 mW. We have recorded a beat note between the first two optical sidebands of width 1 Hz at 6.834 GHz (corresponding to the hyperfine splitting of the ^{87}Rb ground state). This technique enables the generation of two high-power phase-locked beams for coherent manipulation of atomic states.

PACS 42.55.Px · 42.60.Fc · 42.60.By

A. Waxman (✉) · M. Givon · G. Aviv · D. Groswasser · R. Folman
Department of Physics, Ben-Gurion University, Be'er-Sheva 84105, Israel
e-mail: amirwaxm@bgu.ac.il

M. Givon
e-mail: givonme@bgu.ac.il

G. Aviv
e-mail: gal@bgu.ac.il

D. Groswasser
e-mail: davgros@bgu.ac.il

R. Folman
e-mail: folman@bgu.ac.il

1 Introduction

High-frequency modulation of laser beams is important for various fields including atomic physics, metrology, and optical communications. Many applications, such as atomic clocks [1, 2], magnetic sensors [3], and gravity gradiometers [4], require the experimental realization of a Λ-system. This system consists of two coherent laser fields, two hyperfine levels of an atomic ground state, and an excited state. The frequency of the laser beams could be set to resonance with the excited state, as in coherent population trapping (CPT), or far from resonance, as in stimulated Raman transitions. In both cases the beams must be phase locked and with a tunable frequency difference in the range of several GHz (corresponding to the ground state's hyperfine splitting in alkali atoms). Over the years three main methods have been developed for the generation of the two phase-locked beams: direct light modulation, either by acousto-optical modulation (AOM) [5] or electro-optical modulation (EOM) [6, 7], optical phase locking of two lasers [8, 9] and direct current modulation of a laser diode [10]. In this paper we present a significant improvement to the last method enabling the coherent manipulation of atomic (hyperfine) states without the injection of slave lasers.

Modulation of the DC current injected into the laser diode by an AC signal of frequency Ω_m produces optical side bands. The first-order sidebands are then typically injected into slave lasers for amplification and spectral purification. The final output is two phase-locked laser beams with a frequency difference of $2\Omega_m$. One drawback of such a setup with slave lasers is its complexity. An additional problem is that at high modulation frequencies the injection signal becomes extremely low due to the fact that the modulation response of an edge-emitting diode decreases sharply as the modulation frequency increases.

Published online: 14 January 2009

An alternative method is to modulate the current of a vertical-cavity surface-emitting laser (VCSEL) [11] which is much more susceptible to high-frequency modulation but has very little power (a total of 2 mW).

In the following we exhibit experimental results demonstrating the modulation-response enhancement of an anti-reflection-coated (AR-coated) edge-emitting laser diode in an external cavity. By nearly eliminating the internal cavity of the laser diode and matching the modulation frequency to the free spectral range (FSR) of the external cavity we enhance the modulation index to the point of almost complete carrier suppression even at high modulation frequency. The result is a tunable modulation source in the range of 2.5 to 5.5 GHz, with more than 60% of the total power of the output beam concentrated in the two first optical sidebands.

The modulation enhancement by an external cavity with a mode spacing corresponding to the desired modulation frequency was already reported both for edge-emitting diodes [12] and VCSEL [13]. However, as the internal cavity of the diode was not eliminated in these experiments, a complete carrier suppression was not demonstrated.

In this work we study in detail the effect of cavity length and DC current on the modulation response. We also compare the modulation response of a diode having an internal Fabry–Perot cavity (FP diode) with that of the AR-coated diode, to illustrate the effect of the elimination of the internal cavity. Finally, we demonstrate the efficiency of the method by recording a beat note of the modulated light at 6.834 GHz corresponding to the hyperfine splitting of the ^{87}Rb ground state.

2 Experiment

A diagram of the experimental setup is shown in Fig. 1. Our laser is an external-cavity laser diode (ECLD) in the Littrow configuration. The laser diode is AR-coated (Eagleyard Photonics EYP-RWL-0780-00100-1000-SOT01). The diffraction grating (Spectra Physics, 1800 grooves per mm) is mounted on a piezoelectric transducer providing fine tuning and frequency scan. The first-order diffraction efficiency of the grating, at 780 nm, is around 65%, and the blaze angle is 45.25 degrees. The piezoelectric transducer itself is attached to a 25 mm range translation stage. A microwave signal generator (maximum power of 20 dBm) provides the modulation, which is superimposed with the diode's DC current via a 2.5–6 GHz Bias T (Mini Circuits). The combined signal is then fed to the laser diode along a 50 Ω microstrip transmission line. The laser wavelength during all measurements was 780 nm corresponding to the ^{87}Rb D2 line. The DC current injected to the diode was kept at approximately 45 mA (at this point the modulation response was optimal).

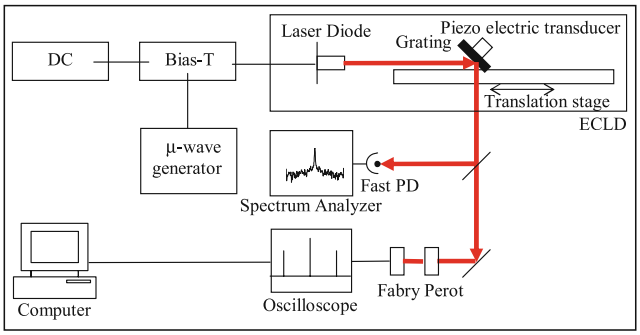

Fig. 1 The experimental setup. A microwave signal generator provides the modulation, which is superimposed with the diode's DC current via a 2.5–6 GHz Bias-T. The combined signal is then fed to the laser diode along a 50 Ω microstrip transmission line. The external cavity length is controlled by the translation stage and its micrometer screw, and the piezoelectric transducer which provides fine tuning. The spectrum of the modulated signal is monitored by a scanning Fabry–Perot. Since the modulation frequency exceeds the FSR of the Fabry–Perot (1 GHz), we used a computer program to "unfold" the recorded spectrum

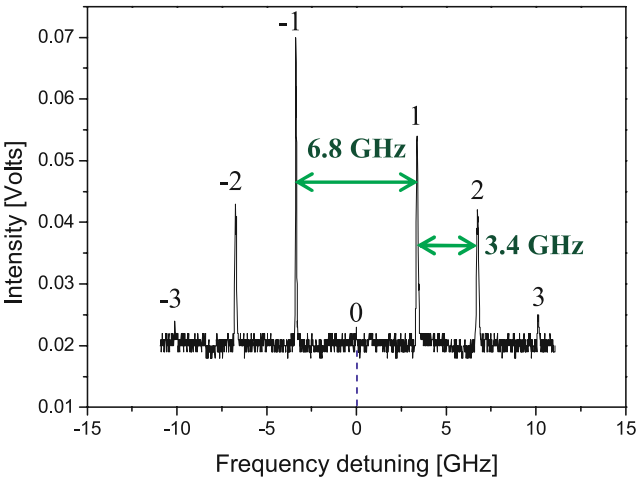

Fig. 2 The emission spectrum of the modulated AR-coated laser diode. The carrier (detuning zero) is completely suppressed. Note the asymmetry between the upper and lower side bands (see (4) and (5)). The best achieved with a FP diode was $\frac{I_1}{I_0} \sim 1$, where I_1 and I_0 are the sideband intensity and carrier intensity, respectively

The microwave power in the various experiments was between 15 and 20 dBm. It was kept fixed during each measurement of the modulation response as a function of the modulation frequency.

The frequency modulation (FM) spectrum of the laser beam is detected by a scanning Fabry–Perot interferometer with an FSR of 1 GHz and is monitored on an oscilloscope. The FM spectrum is analyzed by a computer program to locate the peaks, unfold the folded 1 GHz spectrum, and calculate the modulation index (see Fig. 2).

Modulating the current injected into the diode with a sine wave will induce a phase in the electric field:

$$E = E_0 e^{i[\omega t + m\sin(\Omega t)]}, \tag{1}$$

where m is the modulation index and Ω is the modulation frequency. Expanding (1) and using Fourier components leads to

$$E = E_0\left(\sum_{k=0}^{\infty} J_k(m)e^{ik\Omega t} + \sum_{k=0}^{\infty}(-1)^k J_k(m)e^{-ik\Omega t}\right)e^{i\omega t}, \tag{2}$$

where J_k is the Bessel function of the first kind of order k representing the amplitude of the k^{th} sideband. In particular, J_0 is the amplitude of the carrier (the component with the unmodulated frequency).

An example of the (unfolded) FM picture is shown in Fig. 2. The modulation index can be calculated from the spectrum using

$$\frac{I_1}{I_0} = \frac{J_1(m)^2}{J_0(m)^2}, \tag{3}$$

where I_1 and I_0 are the intensities of the peaks representing the first sideband and the carrier respectively.

As seen in Fig. 2 there is sometimes an asymmetry of the sideband intensity. This indicates amplitude modulation of the laser's radiation [14]. The intensity of the lower and upper sidebands then reads, respectively,

$$I_1 = \left[J_1(m) + (M/2)J_2(m) + J_0(m)\right]^2 {E_0}^2, \tag{4}$$

$$I_{-1} = \left[-J_1(m) + (M/2)J_2(m) + J_0(m)\right]^2 {E_0}^2. \tag{5}$$

From these two equations the AM modulation index M and the FM modulation index m may be calculated. Alternatively, using (3) and replacing I_1 with the average value of the two sidebands gives a reasonable estimation of the FM modulation response.

3 Results

While modulating the diode laser's current, the modulation response increases dramatically at certain modulation frequencies. By scanning the modulation frequency we were able to improve the modulation depth from almost no carrier suppression to full carrier suppression. This is demonstrated in Fig. 2. Alternatively, we can determine the frequency of the modulation response peak by changing the cavity length as shown in Fig. 3. From the graph it is clear that the maximal modulation depth is obtained whenever the modulation frequency corresponds to the FSR resonance condition of the cavity given by

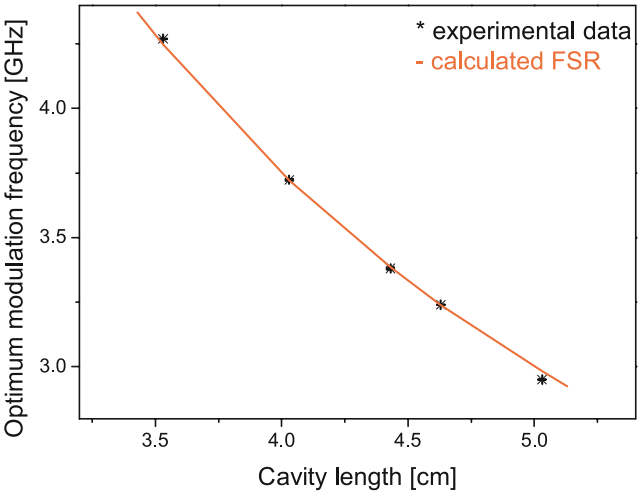

Fig. 3 The effect of the cavity length on the modulation response. For every cavity length we searched for the strongest modulation response. The experimental data are fitted to the theoretical formula $\text{FSR} = c/2L_{\text{eff}}$. The error bars are too small to be shown on this scale. In this work we focus on this optimal configuration in which the modulation frequency equals the FSR

$$\text{FSR} = \frac{c}{2L_{\text{eff}}}, \tag{6}$$

where L_{eff} is the effective cavity length given by

$$L_{\text{eff}} = L_{\text{diode}}n_{\text{diode}} + L_{\text{ext}}n_{\text{ext}}. \tag{7}$$

Here n_{diode} and n_{ext} are the refractive indices of the diode's active medium and air, respectively.

One may conclude that the optical sidebands are enhanced when they are supported by the external cavity modes. The width of these modes will determine the width of the modulation response peak.

The complete picture is revealed when we scan the modulation frequency over a wide range. At low frequencies (200–600 MHz) the diode is susceptible to modulation. As we increase the modulation frequency the sidebands decay. The modulation index is suddenly increased again when the modulation frequency is around the value of half the FSR. This is shown in Fig. 4. It is important to mention that at this point only the second optical sidebands are observed. The first sidebands are suppressed since they do not overlap the cavity modes. The modulation index at this point is lower relative to the full FSR case indicating that the carrier is not fully suppressed. Scanning further, the modulation response decays only to revive again when the modulation frequency matches the FSR. At this point, sidebands from both odd and even orders will appear as they are all supported by the cavity modes.

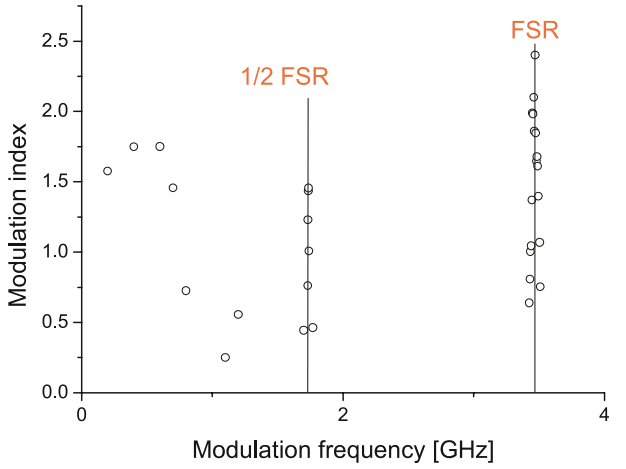

Fig. 4 The modulation response (represented by the modulation index) along a wide spectrum of modulation frequencies is shown for a fixed cavity length. The *open circles* represent the experimental data, while the vertical lines denote the modulation frequencies corresponding to half and full FSR of the external cavity. For calculating the modulation index around the FSR we use (3) and the values of I_0, I_1, and I_2 (note that the $J_0(m)$ Bessel function goes to zero at $m = 2.4$, and hence the FSR peak height of 2.4 indicates full carrier suppression). For calculating the modulation index around $\frac{1}{2}$FSR we replace I_1 and J_1 in (3) with I_2 and J_2 respectively, as I_1 does not exist

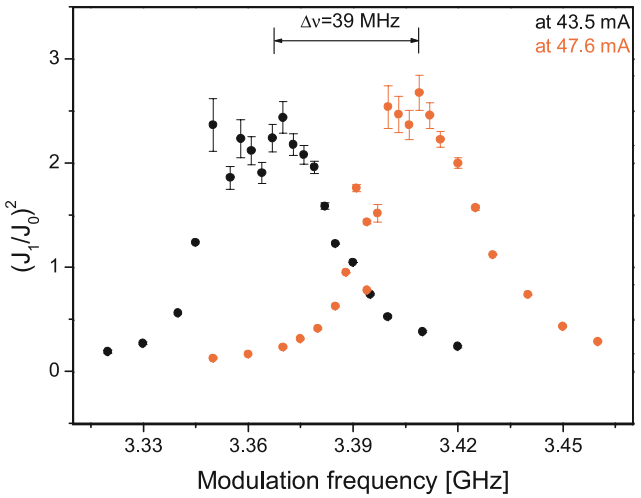

Fig. 5 The modulation response for two current values, for a fixed cavity length. The modulation frequency peaks differ by 39 MHz exhibiting the dependence of the modulation response on current. The large errors around the peaks result from negligible values of J_0

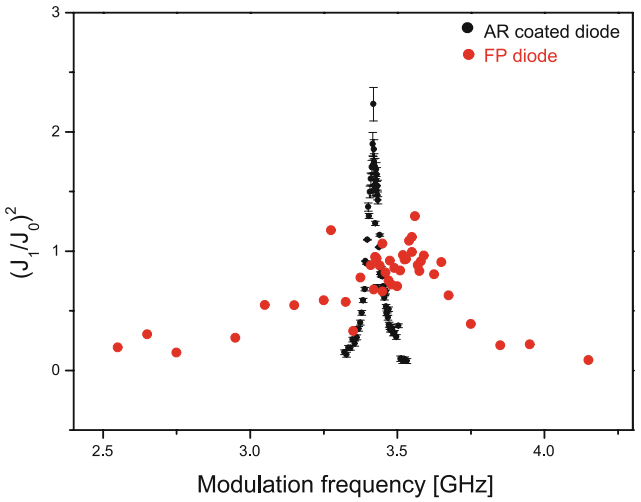

Fig. 6 A comparison between the modulation response of AR-coated and FP diodes (for a fixed current). The external cavity length in both measurements was approximately the same (differences of several hundreds of microns may occur due to the different packages of the diodes). A much larger ratio between the $(\frac{J_1}{J_0})^2$ of the two diodes is achieved when the current is optimized leading to the difference noted in Fig. 2

We were able to demonstrate modulation enhancement up to 5.5 GHz. The modulation efficiency decreases for higher frequencies as the Bias-T we use has a frequency-dependent transmission: We measured a 10 dB attenuation of the power injected into the diode at microwave frequency of 6 GHz comparing to the power injected at 3 GHz. Improvement in the electronics may enlarge the modulation range.

Another important parameter is the DC current. Increasing the injection current will reduce the ratio (I_m/I_0) between the modulating current and the DC current leading to a decrease of the modulation index. Such a behavior was already reported in [14].

In our system we observed an additional phenomenon relating to the current: The frequency of the modulation peak can be controlled by the variation of the current. This is shown in Fig. 5. A difference of 39 MHz in the modulation peak is achieved by a current shift of 4 mA. While the translation stage enables us to match the cavity's FSR to the required modulation frequency in the range of GHz, we can finely tune the FSR with the piezoelectric transducer, and we can also use the current for auxiliary tuning. It seems reasonable to assume that this behavior is due to the fact that the change of current affects the refraction index of the diode's active medium leading to a change in the effective cavity length. We intend to investigate further the connection between the current and the modulation depth in order to achieve a quantitative description of this phenomenon.

As noted previously, the modulation enhancement is related to the elimination of the diode's internal cavity by the AR coating. We experimentally tested the modulation response differences between AR-coated and regular FP diodes, and the results are summarized in Fig. 6. The measurements were done without changing the cavity length. The results show that although the modulation depth is enhanced around the same frequency, the response peak of the FP diode is less pronounced. As the distance between the first sidebands, 6.8 GHz, is of the same order as the width

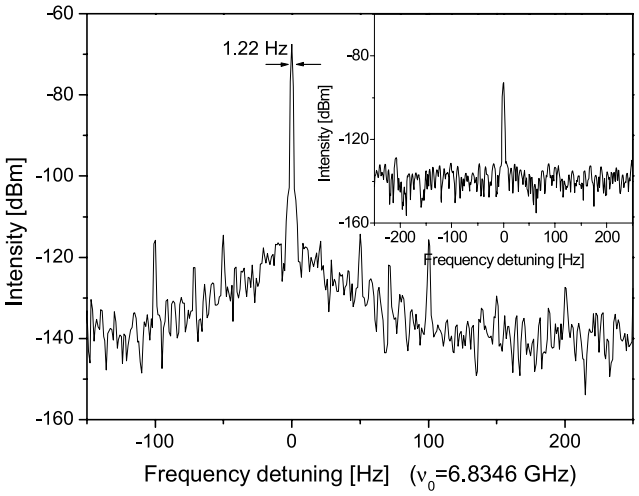

Fig. 7 The frequency beat note between the side bands of the modulated beam. The beat note was measured by a fast photodiode (10 GHz) and analyzed by a spectrum analyzer (stabilized by an external 10 MHz Rb frequency standard). The narrow linewidth of 1.22 Hz, probably limited by the measurement device, is evidence of phase locking. *Inset*: a beat note was recorded at the same frequency, but this time the cavity length was decreased by 2 mm. As a result, the signal is attenuated by 30 dB which exhibits the essence of our findings

of the FP diode transmission peak, and the FP diode cavity FSR is ∼150 GHz, the sidebands' intensity is reduced, and full carrier suppression is not possible.

To show the efficiency of our method in generating two phase-locked beams for atomic coherence experiments, we recorded a single beam beat note of 6.834 GHz (Fig. 7) between the first two optical sidebands. The signal obtained at the modulation frequency (3.417 GHz) was attenuated by 5 dB compared to the former signal indicating the concentration of power in the ±1 sidebands. A slight change of 2 mm in the cavity length attenuates the 6.834 GHz signal by 30 dB as is shown in the inset of Fig. 7.

4 Summary and outlook

We have demonstrated enhancement of the modulation response of an AR-coated laser diode in an external cavity as a function of the cavity length. The peak modulation frequency is tunable in a range of several GHz. A fine tuning of the modulation depth can be made both with the piezoelectric transducer and with the diode's injection current. Our system enables the generation of two coherent laser frequencies without injection locking, as exhibited by the 6.834 GHz beat note in Fig. 7.

The ability to suppress the carrier opens a wide range of applications. For example, injection locking of slave lasers can be used to lock the laser on the higher-order sidebands, in order to generate a larger frequency difference (more than 10 GHz). By modulating the diode's current with a frequency corresponding to half the FSR we may achieve the same goal, since only the even-order sidebands will be enhanced. Another application is offset locking: We can lock one of the side bands to an atomic transition and then inject other sidebands into slaves to amplify them. This method is useful for experiments involving Raman transitions wherein the detuning from the upper level in the Λ-system has to be much larger than the transition width (the transition width being several MHz while the offset frequency is several GHz).

Acknowledgements We thank the team of the Ben-Gurion University *Atomchip* lab (www.bgu.ac.il/atomlab). We also thank Moshe Shuker from the Technion institute for details on impedance matching. We gratefully acknowledge the support of the European Union, the German Government (DIP and GIF projects), the French Government, the American-Israeli Foundation (BSF), and the Israeli Science Foundation.

References

1. V. Shah, S. Knappe, L. Hollberg, J. Kitching, Opt. Lett. **32**, 1244–1246 (2007)
2. H.S. Moon, S.E. Park, Y. Park, L. Lee, J.B. Kim, J. Opt. Soc. Am. B **23**, 2393–2397 (2006)
3. P. Schwindt, S. Knappe, V. Shah, L. Hollberg, J. Kitching, L. Liew, J. Moreland, Appl. Phys. Lett. **85**, 6409 (2004)
4. N. Yu, J.M. Kohel, L. Romans, L. Maleki, in *Quantum Gravity Gradiometer Sensor for Earth Science Applications, ESTC 2002*, Pasadena, CA (2002)
5. P. Bouyer, T.L. Gustavson, K.G. Haritos, M.A. Kasevich, Opt. Lett. **18**, 649 (1993)
6. M. Kasevich, S. Chu, Phys. Rev. Lett. **69**, 1741 (1992)
7. K. Szymaniec, S. Ghezali, L. Coghnet, A. Clairon, Opt. Commun. **144**, 51 (1997)
8. G. Santarelli, A. Clairon, S.N. Lea, G. Tino, Opt. Commun. **104**, 339 (1994)
9. M.J. Snadden, R.B.M. Clarke, E. Riis, Opt. Lett. **22**, 892 (1997)
10. J. Ringot, Y. Lecoq, J.C. Garreau, P. Szriftgiser, Eur. Phys. J. D **65**, 285 (1999)
11. C. Affolderbach, A. Nagel, S. Knappe, C. Jung, D. Wiedenmann, R. Wynands, Appl. Phys. B, Lasers Opt. **70**, 407 (2000)
12. C.J. Myatt, N.R. Newbury, C.E. Wieman, Opt. Lett. **18**, 649 (1993)
13. N. Gavra, V. Ruseva, M. Rosenbluh, App. Phys. Lett. **92**, 221113 (2008)
14. S. Kobayashi, Y. Yamamoto, M. Ito, T. Kimura, IEEE J. Quantum Electron. **18**(4), 582 (1982)